Structural and Material Analysis of an Electromagnetic Actuator for Pressure Control in an Internal Combustion Engine

Jarosław Mamala, Mariusz Graba, Krzysztof Prażnowski
Opole University of Technology, Department of Vehicles, Mikołajczyka 5, 45-271 Opole

Bronisław Tomczuk, Andrzej Waindok
Opole University of Technology, Department of Electrical Technology and Mechatronics, Prószkowska 76, 45-758 Opole

Abstract: The article describes the process of selecting the design parameters of the electromagnetic actuator, which was used to regulate the compression pressure in the cylinder of an internal combustion engine. The electromagnetic actuator was installed in the timing system of a single-cylinder internal combustion engine, which forced its basic design parameters in terms of force and frequency of operation. For the electromagnetic actuator in question, field calculations of the esign variants of the linear electromagnetic actuator for two types of materials were conducted. The finite element method was applied to the computer-aided design of electromagnetic actuators. The influence of the magnetic circuit and the dimensions of the windings on the distribution of the magnetic field were analyzed. The thickness and height of the magnetic field induces, and the dimensions of the stator poles have been changed while maintaining the same external dimensions of the actuator for design reasons. All this work was aimed at improving the performance of the internal combustion engine in terms of improving efficiency in terms of partial engine loads. In this area, the internal combustion engine is characterized by low efficiency, significantly deviating from the maximum, and at the same time, during normal operation of vehicles is the area most often exploited.

Keywords: electromagnetic actuator, pressure regulation, combustion engine, ferromagnetic material

1. Introduction

Internal combustion engines of vehicles equipped with classic drive systems operate in the part load range, where the engine efficiency is much lower than the maximum [15]. This fact is especially true for urban driving, where the crankshaft speeds of the engine are much lower than in highway driving, and its changes are more frequent and intense. The same applies to the variability of the load of the internal combustion engine in the drive train, as shown in Fig. 1.

Regardless of the driving style, the partial load of the internal combustion engine does not exceed one-third of the engine power in 60 % of the total distance covered in changing road conditions. Regarding variable driving conditions, they determine the set operating point of the internal combustion engine, the efficiency of which directly depends on the compression pressure in the cylinder during its operation. Maintaining the highest compression pressure possible under given conditions for traditional internal combustion engines is difficult due to the limitations of the combustion process of the air mixture in the cylinder, including the occurrence of knocking. In internal combustion engines, the maximum peak compression pressure can be adjusted in several ways. Currently, the most popular method of changing cylinder pressure is to change the throttle opening, which limits the flow of the fuel-air mixture to the engine and the increase in pressure. Reduced flow with the intake manifold throttle closed or partially open, the combustion engine operates with a large negative charge change loop. This leads to an increase in engine resistance, the so-called pumping losses, which of, partial load work amount to up to 12 % [3], which deteriorates its efficiency. One way to solve this problem is to use internal combustion engines with variable compression or operating according to the Atkinson cycle [6, 8, 13]. The change in compression ratio enables the use of a high compression ratio under low load conditions and its low stage under high load conditions of an internal combustion engine. The authors used a combined approach to use an internal combustion engine with an increased compression ratio, and the compression pressure control used an electromagnetic actuator in its timing system.

Autor korespondujący:
Jarosław Mamala, J.Mamala@po.edu.pl

Artykuł recenzowany
nadesłany 23.05.2023 r., przyjęty do druku 17.12.2023 r.

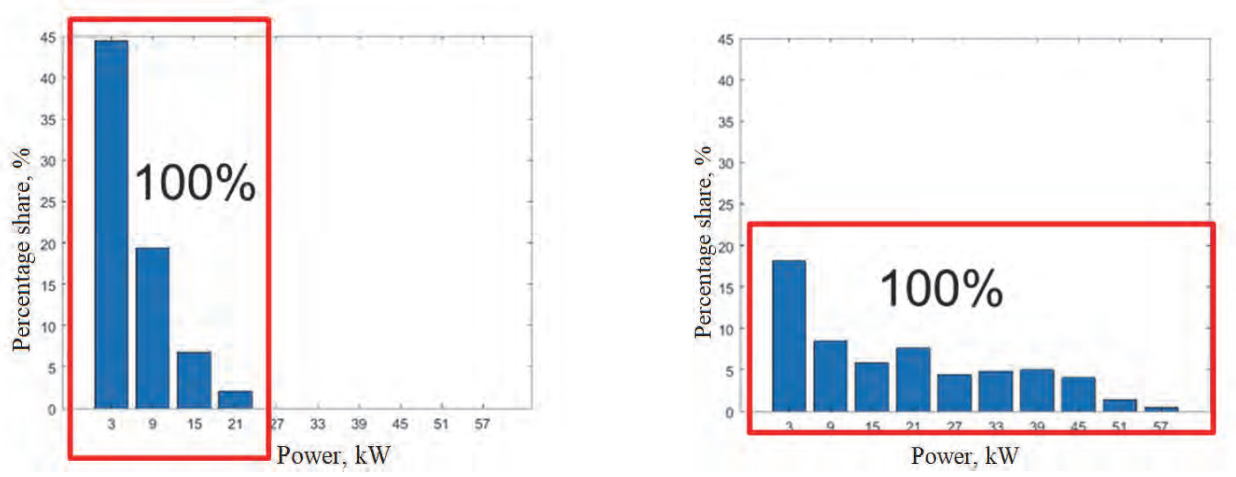

(a) (b)

Fig. 1. Characteristics of the power usage of the internal combustion engine during normal operation for driving: (a) economical, b) dynamic
Rys. 1. Charakterystyka wykorzystania mocy silnika spalinowego podczas normalnej pracy dla jazdy: (a) ekonomicznej, b) dynamicznej

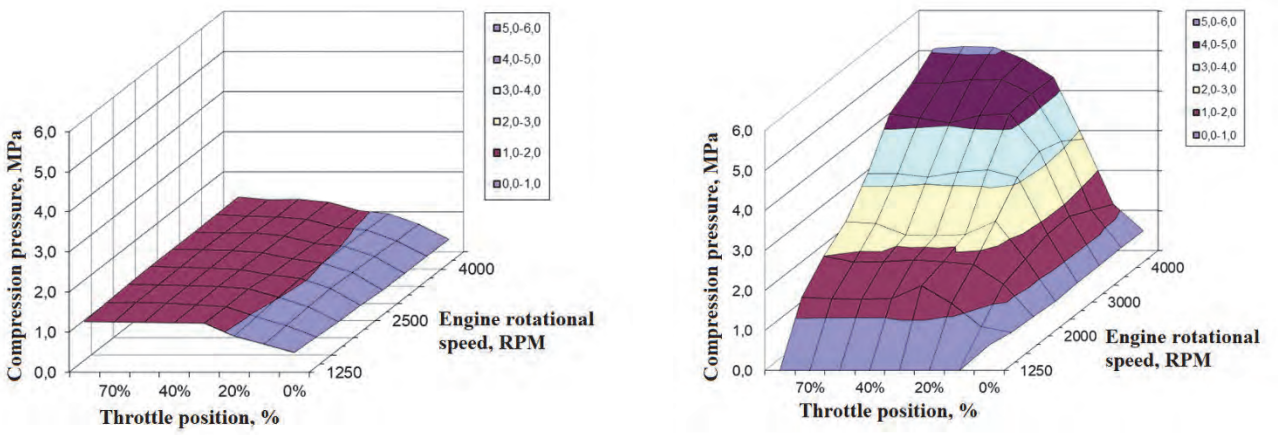

(a) (b)

Fig. 2. Compression pressure characteristics for the internal combustion engine under test: (a) ignition off, b) normal operation
Rys. 2. Charakterystyki ciśnienia sprężania badanego silnika spalinowego: (a) zapłon wyłączony, b) praca normalna

2. Compression pressure in the cylinder

The maximum increase in compression pressure is the basic indicator of the operation of an internal combustion engine, which characterizes its working capacity and is often related to the compression ratio in the engine. In the case of internal combustion engines, its maximum value depends not only on the compression ratio, but also on the throttle tilt, which determines the filling of the cylinder with a fresh load in the compression stroke. The basic characteristics of the change in the maximum compression pressure in the cylinder for a single-cylinder internal combustion engine are shown in Fig. 2.

A significant qualitative and quantitative difference can be seen comparing the compression pressure characteristics in the cylinder for an internal combustion engine with the ignition OFF (Fig. 2a) with the characteristics with the ignition ON (Fig. 2b).

Figure 2b shows a pressure increase of more than five times, and its significant increase occurs after exceeding 2500 rpm, in this range the internal combustion engine does not have good efficiency.

Hence, the compression ratio has been increased in the test combustion engine, and a new solenoid actuator has been added to the timing system to control the intake valve to improve efficiency. The solenoid actuator drives the valve and performs the normal operation of the intake valve, and in the higher speed range, the opening time is extended, which reduces the filling of the cylinder with fresh load and consequently reduces the pressure in the cylinder [14–16]. Such electromagnetic actuators are used in many applications, e.g., for transport [1, 2], wave-energy conversion [4] and linear motors [5, 7]. Their use eliminates the conversion of rotational motion into linear motion as in the case of the timing system of internal combustion engines, and is characterized by high reliability, good dynamic properties, and electromechanical parameters [9]. The electromagnetic actuator built into the timing system is shown on the engine (Fig. 3).

3. Electromagnetic actuator

Due to the specificity of the actuator installation site and limited dimensions, a tubular structure was chosen for further analysis, calculations, and simulation of the magnetic field. It is the most effective structure in terms of the ratio of electromagnetic force to the mass of the moving element [11, 12]. Figure 4 illustrates an actuator with the main dimensions marked. This model was used in a simulation program.

An electromagnetic actuator consists of a stator and a mover. In the first stage of calculations, the preliminary number of turns was assumed. The polarization field is excited by currents in the external coils. Their main task is to keep the drive in stable, extreme positions (valve open and closed), and each of them has $N_1 = 72$ turns. The controlled electromagnetic field is produced by two internal coils with $N_2 = 118$ turns each. The main task is

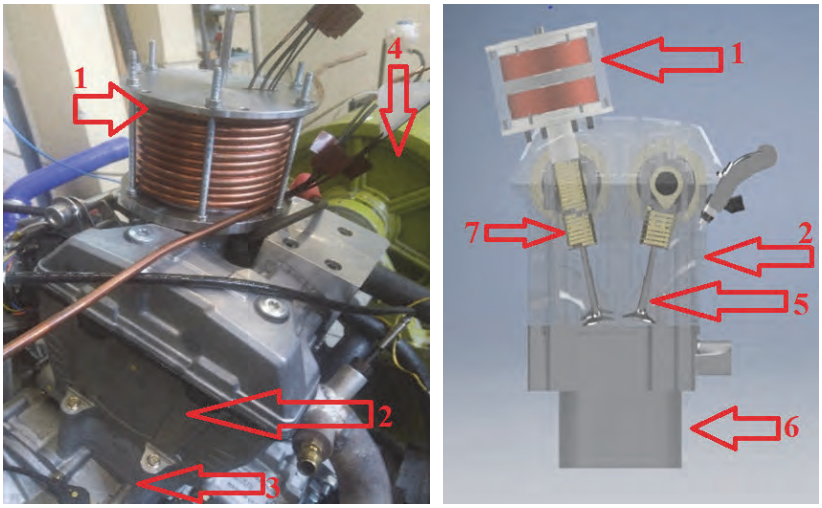

(a) (b)

Fig. 3. Single-cylinder internal combustion engine with electromagnetic actuator: (a) actuator built on the engine with cooling system, (b) method of mounting the actuator on the cylinder head (1 – electromagnetic actuator, 2 – cylinder head, 3 – engine, 4 – dynamometer, 5 – engine valves, 6 – cylinder, 7 – spring)
Rys. 3. Jednocylindrowy silnik spalinowy z siłownikiem elektromagnetycznym: (a) siłownik zabudowany na silniku z układem chłodzenia, (b) sposób mocowania siłownika na głowicy (1 – siłownik elektromagnetyczny, 2 – głowica, 3 – silnik, 4 – hamownia, 5 – zawory silnika, 6 – cylindrowy, 7 – sprężyna)

Table 1. Initial dimensions of cylinder parts (in mm)
Tabela 1. Początkowe wymiary części cylindra (w mm)

Dimension	R_s	R_o	R_z	R_i	h_z	h_g	h_p	h_r	g	h_C	w_{c1}	w_{c2}	h_s	w_s
Value	42	8.5	8	3	8	6	8	40	0.5	27	16.5	10	29	4

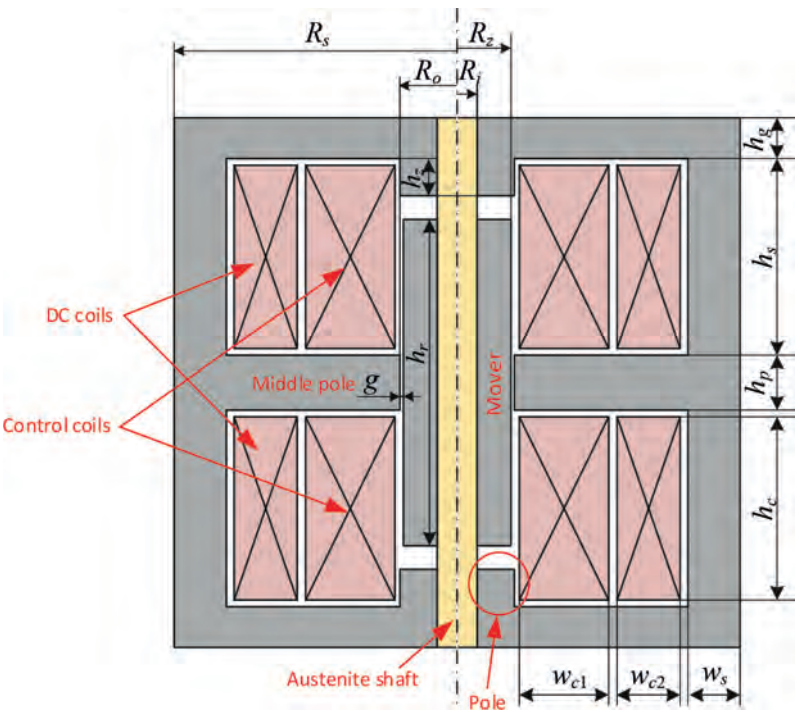

Fig. 4. Model used in the simulation program in axial cross-section with defined basic dimensions
Rys. 4. Model zastosowany w programie symulacyjnym w przekroju osiowym z określonymi wymiarami podstawowymi

to move the core and stabilize it in each position. A cross-section of the wire without insulation (3 mm^2) and the dimensions of the coils were used to calculate the number of turns. The stator consists of the main outer part of the tube shape, as well as the bottom and top covers, which form the main magnetic circuit. The drive consists of two parts: the shaft and the ferromagnetic mover. In the analysis of the distribution of the magnetic field, austenite shafts were also considered. Table 1 gives the initial dimensions for the cylinder variant calculations.

4. Mathematical model for magnetic field analysis

The distribution of the magnetic field was modelled using FEM software, and to simplify field analysis in the mathematical model, eddy currents were omitted, and the magnetic field is considered stationary. In addition, the fact that the manufacturing process slightly changes the magnetic properties of the core material is not considered. Therefore, in the calculations, the value of the magnetic air gap in the calculation model was slightly increased. However, the nonlinear nature of flux density changes as a function of field strength was considered, and it was assumed that the problem of the magnetic field in the 3D dimension can be reduced to a 2D problem, which significantly simplifies the mathematical description of the model and shortens the calculation time. This is due to the geometry of the object under study since the structural details do not significantly affect the distribution of the magnetic field. Thanks to this, two-dimensionality makes the calculations representative. Assuming, as in [11], the nonlinear nature of magnetization in pieces of a ferromagnetic core the magnetic field can be described by the following formula (1):

$$\nabla \times \left(\frac{1}{\mu(B)} \nabla \times \mathrm{A} \right) = J. \tag{1}$$

The field analysis is based on the calculation of the magnetic vector potential A [4], which has only the polar component of the vector (A_φ). Due to the cylindrical symmetry of our tubular actuator, for which a polar coordinate system is used. When the polar component of the vector potential is used (as a function of finding) [12], the magnetic field can be described by the following partial differential equation (2):

$$\frac{\partial}{\partial r}\left(\frac{1}{\mu(B)} \frac{\partial A_\varphi}{\partial r} \right) + \frac{1}{r\mu(B)} \frac{\partial A_\varphi}{\partial r} + \frac{\partial}{\partial z}\left(\frac{1}{\mu(B)} \frac{\partial A_\varphi}{\partial z} \right) - \frac{1}{\mu(B)} \frac{\partial A_\varphi}{r^2} = J_\varphi \tag{2}$$

where $\mu(B)$ is the nonlinear permeability of the magnetic material and J is the current density in the excitation windings.

Given the potential rotation operator, it is possible to calculate the components of the magnetic flux density vector.

$$B = -\frac{\partial A_\varphi}{\partial z}\mathbf{1}_r + \frac{1}{r}\frac{\partial (rA_\varphi)}{\partial r}\mathbf{1}_z. \tag{3}$$

Based on the knowledge of the distribution of the magnetic field, its integral parameters can be determined, including the magnetic force generated by the actuator is particularly important. The force was determined by Maxwell's surface stress tensor [4] at the edge of a moving ferromagnetic region:

$$\mathrm{F}_e = \int_\Omega f \, d\Omega = \oint_\Gamma \ddot{\mathrm{T}} \cdot d\Gamma, \tag{4}$$

where:

$$\ddot{\mathrm{T}} = \begin{bmatrix} \mu\left(H_r^2 - \frac{1}{2}H^2 \right) & \mu H_r H_z \\ \mu H_r H_z & \mu\left(H_z^2 - \frac{1}{2}H^2 \right) \end{bmatrix}. \tag{5}$$

Another important integral parameter that affects the inductance of the actuator is the magnetic flux Ψ associated with all turns of the winding. For the k-th winding, we can calculate the product of the normal component $\mathrm{B_n}$ and the area of each element within the surface circled by the contour of the turn. After integrating such products on each turn of the winding and summing the integrals, the flux bond can be determined.

$$\Psi = \sum_{k=1}^{N} \int_S B_n \, dS_k, \tag{6}$$

where: S_k – the area enclosed by *the* c^{th} coil.

The dynamic inductance of a coil was calculated by definition as the partial derivative of the connection of the flux associated with the coil relative to the current

$$L_d = \frac{\partial \Psi}{\partial i}. \tag{7}$$

The presented formulas (1)–(7) are used by the simulation program for calculations to check the field at any points, as well as evaluate many different integrals and plot various interesting quantities along the contours defined by the user (Fig. 4). The nonlinear curve $B(H)$ is included in the model. For the outer boundaries of the computational area, the zero Dirichlet condition ($A_\varphi = 0$) was used.

5. Calculation results

Assuming additional cooling of the main actuator body (external magnetic core), high values of current density $J = 10$ A/mm^2 in all coils were assumed. For polarization and control coils, the initial height h_c was the same. The initial thickness of the control coil in c_1 and the polarization coil in c_2 is given in Table 1. For the initial dimensions, the same value of $I = 30$ A of the current in the bias and control coils was assumed.

5.1. Influence of dimensions (R_z) on actuator parameters

Strong changes in the integral parameters of the magnetic field occur in the event of an increase in the volume of the moving ferromagnetic core. The diagrams below (Fig. 5 and 6) show the dependence of changes in radius R_z form a moving element on the thrust value vs. mover position. Due to the constancy of the volume of the actuator, it is obvious that an increase in the radius causes a decrease in the thickness of the coils.

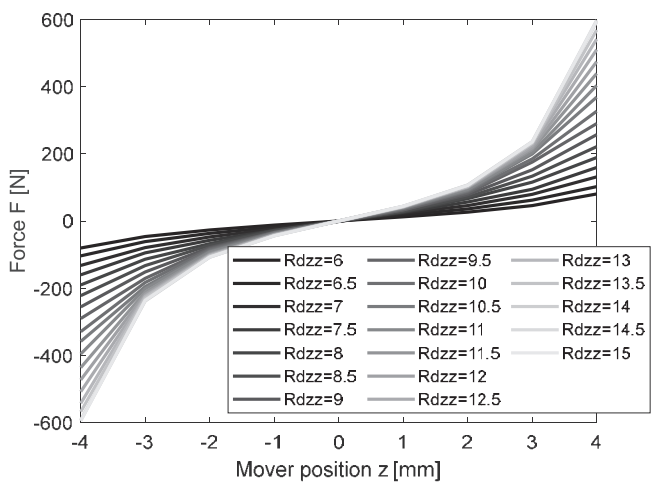

(a)

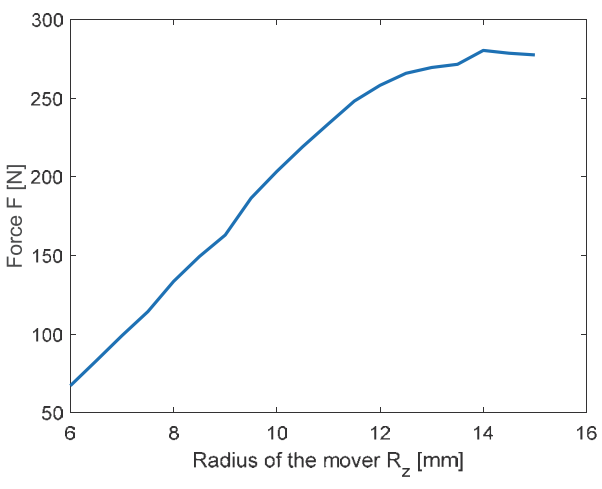

b)

Fig. 5. (a) Dependence of the thrust value vs. mover position for I_{DC} = 30 A and I_c = 0 for different R_z values [in mm]; (b) The thrust vs. radius of the mover for z = 0, I_{DC} = 30 A and I_c = 30 A

Rys. 5. (a) Zależność wartości ciągu od położenia rdzenia dla I_{DC} = 30 A i I_c = 0 dla różnych wartości R_z [w mm]; (b) Siła ciągu w funkcji promienia rdzenia dla z = 0, I_{DC} = 30 A i I_c = 30 A

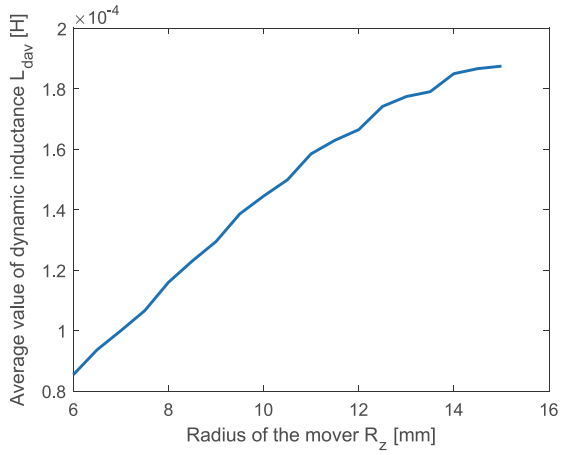

Fig. 6. Dependence of the mean dynamic inductance R_z value
Rys. 6. Zależność średniej indukcyjności dynamicznej od wartości R_z

Considering the realistic dimensions of the actuator, the radius R_z has been changed from 6 mm to 15 mm. Therefore, for this range, the graphs of the force value vs. mover position for $I_{DC} = 0$ and force value for $z = 0$ ($I_{DC} = 30$ A and $I_c = 30$ A) are given in Figures 5a and 5b, respectively. In the case of a 2-fold increase in this radius, a 4-fold increase in the force value is observed. However, there is a maximum (for $R_z = 14$ mm) of the observed force value (Fig. 5b).

The obtained results show that the radius of the moving element significantly affects the average value of the dynamic inductance L_{dav} (Fig. 6). The negative effect of the radius R_z is such that it increases the inductance of L_{dav}.

5.2. Influence of ratio wc2/wc on actuator parameters

Figure 7a shows the force value vs. mover position for different values of ratio w_{c2}/w_c ($I_{DC} = 30$ A). In Figure 7b the force value for $z = 0$ ($I_{DC} = 30$ A and $I_c = 30$ A) vs. ratio w_{c2}/w_c is presented. The ratio was changed from 0.3 to 0.72. External dimensions of the actuator were kept constant. It is visible, that the ration w_{c2}/w_c slightly influences the force value for $z = 0$ – there is a 34 % difference between the highest (134 N for $w_{c2}/w_c = 0.5$) and lowest (100 N for $w_{c2}/w_c = 0.3$) value. The highest value is obtained for $w_{c2}/w_c = 0.5$, which means that the best solution is to keep the width of the DC coils and control coils equal.

6. Experimental research

For the control of the electromagnetic actuator, an interface was made in the LabVIEW program on the CompactRio platform cooperating with the motor ECU so that the actuator could be adjusted, as shown in Figure 8.

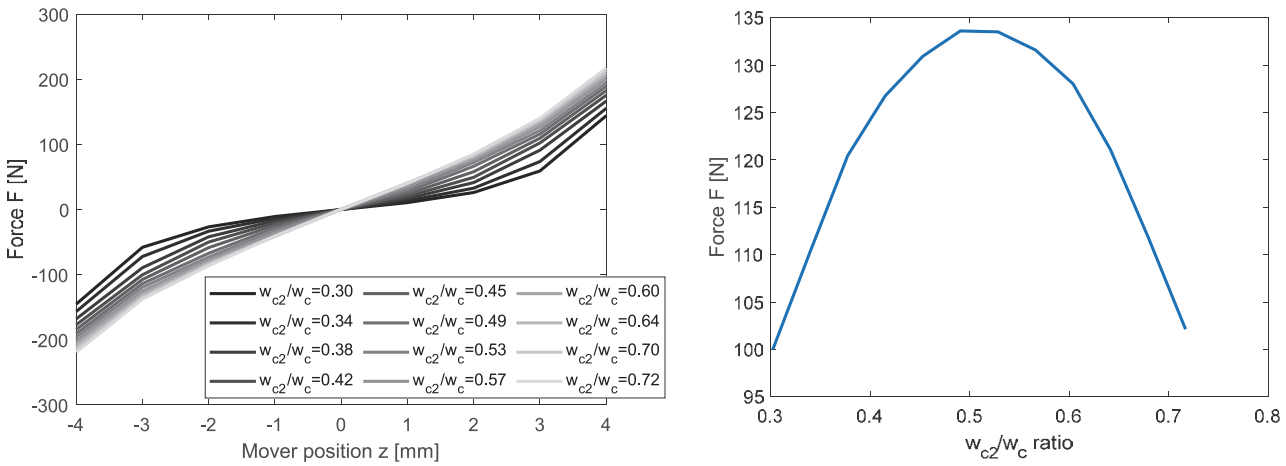

(a) b)

Fig. 7. (a) Dependence of the thrust value vs. mover position for I_{DC} = 30 A and I_c = 0 for different w_{c2}/w_c values; (b) The thrust vs. radius of the mover for z = 0, I_{DC} = 30 A and I_c = 30 A
Rys. 7. (a) Zależność wartości ciągu od położenia rdzenia dla I_{DC} = 30 A i I_c = 0 dla różnych wartości w_{c2}/w_c; (b) Siła ciągu w funkcji promienia rdzenia dla z = 0, I_{DC} = 30 A i I_c = 30 A

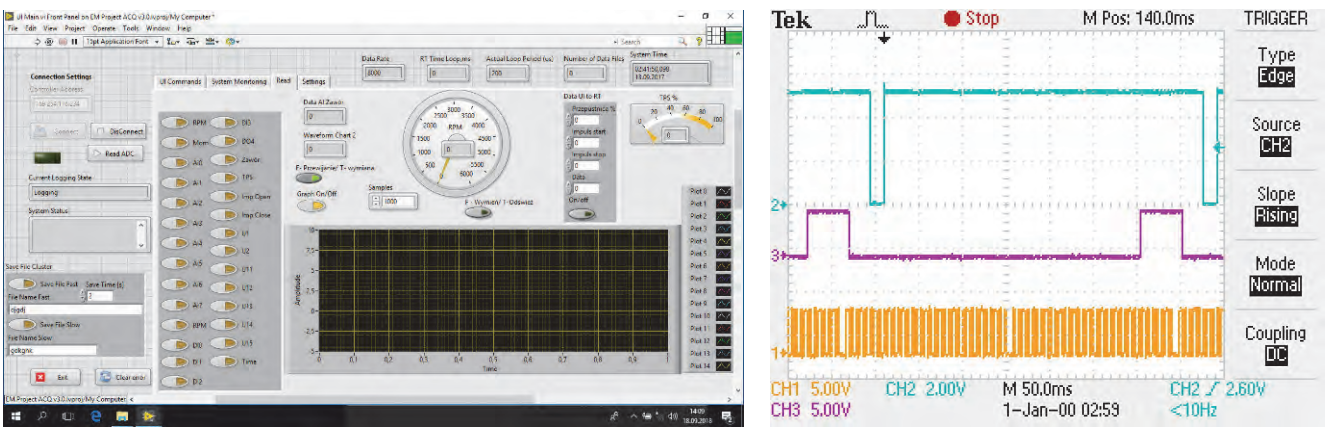

Fig. 8. Electromagnetic actuator control interface: (a) LabVIEW interface, (b) signals recorded from the internal combustion engine under test: orange for camshaft, purple for fuel injector, green for engine GPM
Rys. 8. Interfejs sterujący siłownikiem elektromagnetycznym: (a) interfejs LabVIEW, (b) sygnały rejestrowane z badanego silnika spalinowego: pomarańczowy – wałka rozrządu, fioletowy – wtryskiwacza paliwa, zielony – GPM silnika

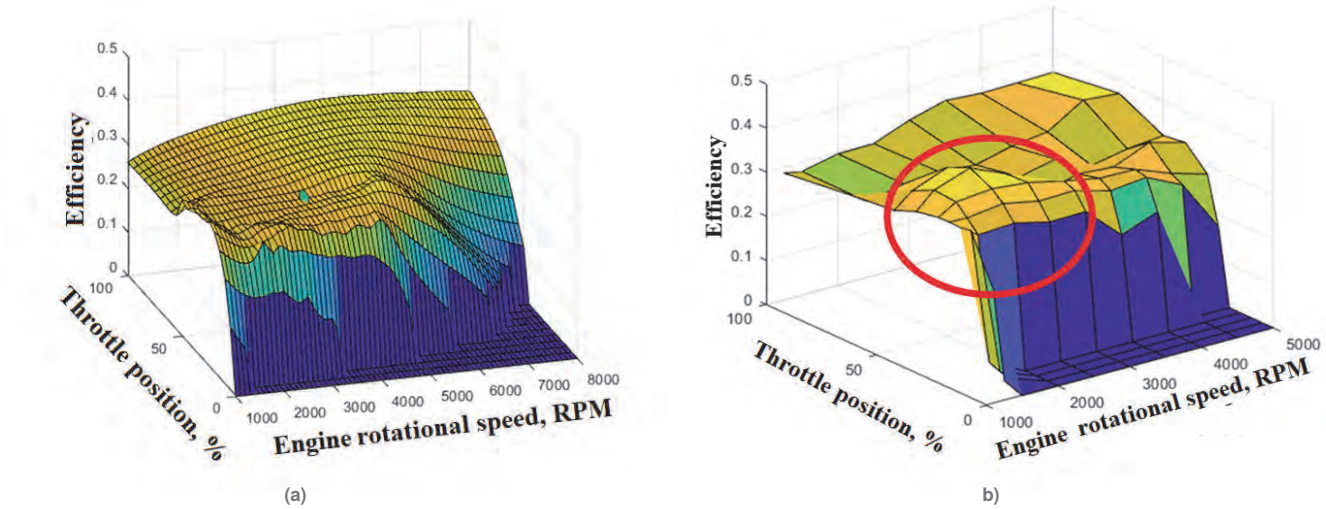

Fig. 9. Efficiency characteristics for the internal combustion engine under test: (a) for a series engine with a compression ratio of 9.2 : 1, (b) an engine with a modified timing system and a compression ratio of 11,5 : 1
Rys. 9. Charakterystyki sprawności badanego silnika spalinowego: (a) dla silnika seryjnego o stopniu sprężania 9,2 : 1, (b) silnika ze zmodyfikowanym układem rozrządu i stopniem sprężania 11,5 :1

The advantage of this system, in addition to the high speed of operation, is also the possibility of constant and simple correction of control parameters. This system reads signals from the engine, i.e., camshaft and crankshaft signals, and on their basis and software variables, generates a control signal for the actuator (Fig. 8b). Tests checking the operation of the system were conducted on the engine dynamometer, which is equipped with the Department of Vehicles of the Opole University of Technology.

The greatest efficiency improvement for the engine under test occurs in the engine part load range at low engine speeds not exceeding 2500 rpm. In this area, the available power of the internal combustion engine does not exceed one-third of the maximum power, as in the case of Figure 1. The efficiency gain in this area is indicated by a red wheel in Figure 9. In the marked characteristic area, the efficiency of the motor increases by up to 25 %, and this is due to the improvement of the compression pressure in the low-load range. The presented efficiency characteristics are shown only in the range of limited crankshaft speed of the internal combustion engine up to 4000 rpm. At higher speeds of the internal combustion engine, the frequency of the actuator operation, with a supply voltage of 12 V from the vehicle's electrical system, is insufficient. Hence, a theoretical analysis was made for another ferromagnetic material in the form Somaloy [10], according to the presented calculation scheme. It is a composite material made of ferromagnetic powders with suitable properties.

7. Actuator made of steel ST3 and Somaloy

For the theoretical analysis of the electromagnetic actuator prototype, assumptions were made in the form of the value of bias excitation current $I_{DC} = 28.35$ A and the number of turns in external coils $N_1 = 77$. For the internal coils (control), the number of turns was equal to $N_2 = 74$. The dimensions of the actuator have been slightly changed due to experimental studies and previous calculations, and new dimensions are given in Table 2. The outer diameter of the actuator and its height have been slightly increased. The other dimensions were close to the initial ones. The thin (6 mm diameter) movable mandrel is made of acid-resistant (austenitic) steel. For such changes, the mass of the actuator drive was 253 g.

Considering the dimensions given in Table 2, the two materials used for the cylinder core are compared below. Steel ST3 core and Somaloy 130i1P [17] composite material with known ferromagnetic properties were compared. Their $B(H)$ curve was given in Figure 10.

On the left side of Figure 11a ($I_c = 0$) you can see that the thrust is smaller for the Somaloy magnetic circuit, and for this material, the maximum magnetic force is 320 N. Comparing the ferromagnetic steel core, the maximum force value is greater and amounts to 525 N. This graph was generated considering only the bias current.

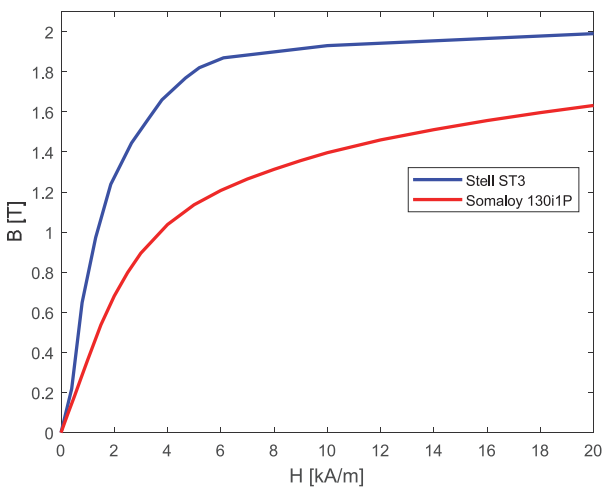

Fig. 10. B(H) curve for steeel ST3 and Somaloy 130i1P
Rys. 10. Krzywa B(H) dla stali ST3 i Somaloy 130i1P

Table 2. New cylinder part dimensions (in mm)
Tabela 2. Zaktualizowane wymiary części cylindra (w mm)

Dimensions	R_s	R_o	R_z	R_i	h_z	h_r	H_C	w_{c1}	w_{c2}	h_s	w_s
Value	50	13.5	13	4 (3)	10	38	28	12	11.5	30	10

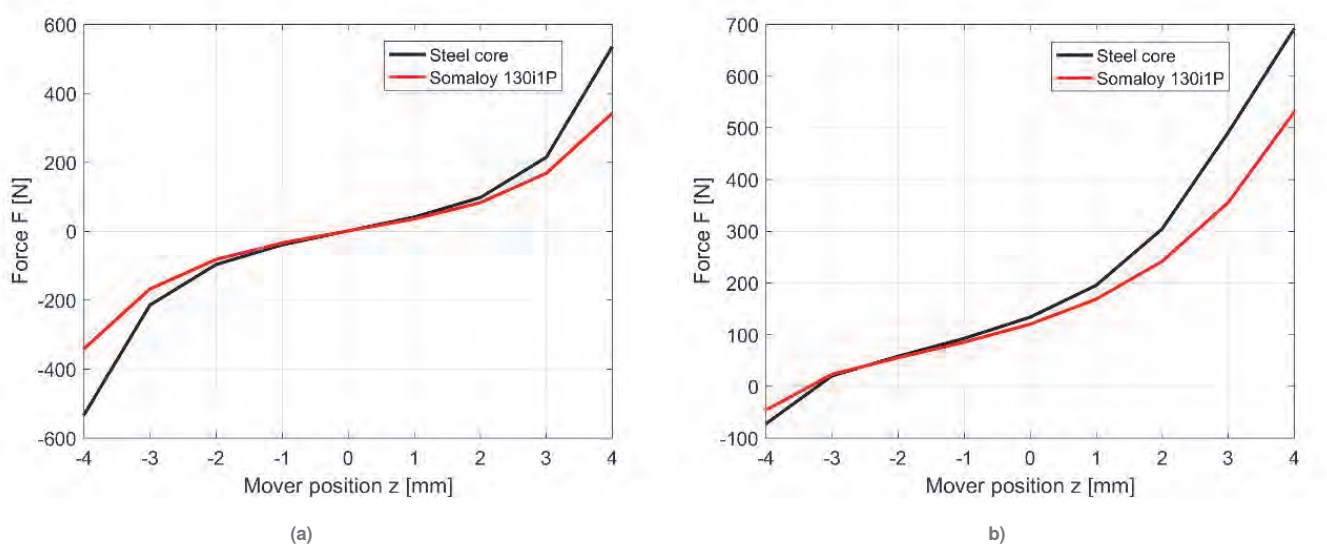

Fig. 11. Dependence of the thrust force of the electromagnetic actuator on the value of the drive stroke, for: a) Ic = 0 A, b) Ic = 15 A
Rys. 11. Zależność siły ciągu siłownika elektromagnetycznego od wartości skoku rdzenia, dla: a) Ic = 0 A, b) Ic = 15 A

On the right side of Fig. 11b you can see that the control current $I_c = 15$ A increases the pulling force (at maximum stroke) to 550 N (for Somaloy) and to 700 N for the steel core. This is due to the sustaining of the DC flux in the outer windings by the control winding flux. Since the control stream is directed in one direction, the graph is not symmetrical according to the $z = 0$ coordinate of the moving motion.

For the application under consideration, the thrust required to open the intake valve by the designed solenoid power plant for the test engine was 400 N. In addition, when the valve is opened by the actuator, it is pressed by compressed air when closing in the compression stroke. These are the values achieved by both actuators, and the issue of particular importance is maintaining high dynamics at a supply voltage of 12 V.

8. Applications

In the case of the electromagnetic actuator under consideration, its use in the timing system of a spark-ignition internal combustion engine combined with a structurally increased compression ratio had a positive effect on the efficiency of the engine in the low load range of the internal combustion engine. The modified combustion engine features improved part-load performance, including increased power while reducing fuel consumption, resulting in improved efficiency by up to 25 %. The challenge described in the paper is to design the structure of an electromagnetic actuator that would be adapted to the operation of the internal combustion engine, its vibrations, temperature, and frequency. Another challenge is the measurement and control of the actuator in real time, resulting from the angle of rotation of the crankshaft of the internal combustion engine. Theoretical analysis and magnetic field calculations allow for the consideration of different design variants of the linear actuator. The use of the numerical analysis method, considering the assumption and simplification in the form of symmetry of the analyzed actuator, allows to obtain reliable results necessary to design such an actuator. Combined with computer-aided design (CAD), it allows you to optimize actuator shapes using variational and iterative calculations. For the actuator under consideration, it is advantageous to make windings of the same diameter for the DC and control windings. It is recommended to use ferromagnetic poles in the form of upper and lower rings with a height $h_z = 10$ mm. The radius of the movable part should be in the range $R_z = 12$–14 mm. Between the upper and lower windings, there should be a ferromagnetic pole. In the case under consideration, the ratio w_{c2}/w_c should be 0.5. The core material strongly influences the thrust value and for the materials considered in the Somaloy core case, the maximum force value is 39 % lower for $I_s = 0$ A and 21 % lower for $I_s = 15$ A compared to a steel core.

The analyzed electromagnetic actuator is characterized by a new functionality that allows to obtain gains in the indicators of the spark-ignition engine without the need to change its design parameters. It also has its limitations in terms of frequency of operation, but also in terms of energy consumption for its operation. Further work is needed in this area. The profits obtained translate directly into an increase in the overall efficiency of the engine. It is also worth noting that during experimental tests, the phenomenon of knocking in the combustion of the engine was not observed.

Acknowledgments

These works were conducted as part of the projects "R+D works on the method of effective power supply of the internal combustion engine" number: RPOP.01.01.00-16-0063/16-00 and the supporting project number RPOP.01.01.00-16-0026/16-00. Projects co-financed by the European Union from the European Regional Development Fund under the Regional Operational Program of the Opolskie Voivodeship for 2014–2020.

References

1. Duan J.A., Zhou H.B., Guo N.P., *Electromagnetic design of a novel linear Maglev transportation platform with finite-element analysis*, "IEEE Transactions on Magnetics", Vol. 47, No. 1, 2011, 260–263, DOI: 10.1109/TMAG.2010.2087388.
2. Lee H.-W., Kim K.-Ch., Lee J., *Review of Maglev train technologies*, "IEEE Transactions on Magnetics", Vol. 42, No. 7, 2006, 1917–1925, DOI: 10.1109/TMAG.2006.875842.
3. Wanhua S., Zhongjie Z., Ruilin L., Yingjun Q., *Development Trends in the Technologies of Automobile Internal Combustion Engines.* "Strategic Study of CAE", Vol. 20, No. 1, 2018, DOI: 10.15302/ J-SSCAE-2018.01.014.
4. Tomczuk B., Waindok A., Wajnert D., *Transients in the electromagnetic actuator with the controlled supplier*, "Journal of Vibroengineering", Vol. 14, No. 1, 2012, 39–44.

5. Bang Y.B., Lee K.M., *Large thrust linear motors for low-duty-cycle operation*, "Mechatronics", Vol. 14, No. 8, 2004, 891–906, DOI: 10.1016/j.mechatronics.2004.05.001.
6. Lee S.H., Yi H.Ch., Han K., Kim J.H., *Genetic algorithm--based design optimization of electromagnetic valve actuators in combustion engines*, "Energies", Vol. 8, No. 11, 2016, 13222–13230, DOI: 10.3390/en81112352.
7. Sun Z.-Y., Li G.-X., Wang L., Wang W.-H., Gao Q.-X., Wang J., *Effects of structure parameters on the static electromagnetic characteristics of solenoid valve for an electronic unit pump*, "Energy Conversion and Management", No. 113, 2016, 119–130, DOI: 10.1016/j.enconman.2016.01.031.
8. Fan X., Chang S., Liu L., Lu J., *Realization and optimization of high compression ratio engine with electromagnetic valve train*, "Applied Thermal Engineering", Vol. 112, 2017, 371–377, DOI: 10.1016/j.applthermaleng.2016.10.039.
9. Gieras J.F., Piech Z.J., Tomczuk B., *Linear synchronous motors*, CRC Press, Taylor & Francis Group, New York 2011, DOI: 10.1201/b11105.
10. Asari A.R., Guo Y., Zhu J.G., *Magnetic properties measurement of soft magnetic composite material* (*Somaloy 700*) *by using a 3-D tester*. AIP Conference Proceedings, 2017, DOI: 10.1063/1.4998386.
11. Waindok A., Tomczuk B., *Reluctance Network Model of a Permanent Magnet Tubular Motor*, "Acta Mechanica et Automatica", Vol. 11, No. 3, 2017, 194–198, DOI: 10.1515/ama-2017-0029.
12. Waindok A., Tomczuk B., *Field analysis and eddy current losses calculation in five-phase tubular actuator*, "Open Physics", Vol. 15, No. 1, 2017, 897–901, DOI: 10.1515/phys-2017-0107.
13. Liu F., Sun B., Zhu H., Hu T., Du W., Li X., Zhang Z., *Development of performance and combustion system of Atkinson cycle internal combustion engine*. "Science China Technological Sciences", Vol. 57, 2014, 471–479, DOI: 10.1007/s11431-014-5474-8.
14. Wurms R. et al., *The new Audi 2.0l Engine with innovative rightsizing – a further milestone in the TFSI Technology* – XXXVI Internationales Wiener Motorensymposium 2015, Vienna 2015.
15. Mamala J., Graba M., Prażnowski K., Hennek K., *Control of the effective pressure in the cylinder of a spark-ignition engine by electromagnetic valve actuator*, "SAE Technical Papers", 2019, 1–9. DOI: 10.4271/2019-01-1201.
16. Woś P., Balawender K., Jakubowski M., Kuszewski H., Lejda K., Ustrzycki A., *Design of affordable multi-cylinder variable compression ratio* (*VCR*) *engine for advanced combustion research purposes*, "SAE Technical Papers", 2012, DOI: 10.4271/2012-01-0414.
17. Höganäs Soft Magnetic Composite Powders, www.hoganas.com/api/Brochure/?pdf=/globalassets/downloads/libary/somaloy_somaloy-1p-material-data_2272hog.pdf#page=1 (Accessed on 5th December 2023).

Analiza konstrukcyjna i materiałowa siłownika elektromagnetycznego służącego do regulacji ciśnienia w silniku spalinowym

Streszczenie: W artykule opisano proces doboru parametrów konstrukcyjnych siłownika elektromagnetycznego, który posłużył do regulacji ciśnienia sprężania w cylindrze silnika spalinowego. Siłownik elektromagnetyczny został zamontowany w układzie rozrządu jednocylindrowego silnika spalinowego, co wymusiło jego podstawowe parametry konstrukcyjne w zakresie siły i częstotliwości pracy. Dla omawianego siłownika elektromagnetycznego przeprowadzono obliczenia porównawcze wariantów konstrukcyjnych liniowego siłownika elektromagnetycznego dla dwóch rodzajów materiałów. Do komputerowego wspomagania projektowania siłowników elektromagnetycznych zastosowano metodę elementów skończonych. Przeanalizowano wpływ obwodu magnetycznego i wymiarów uzwojeń na rozkład pola magnetycznego. Grubość i wysokość indukowanego pola magnetycznego oraz wymiary biegunów stojana zostały zmienione przy zachowaniu tych samych wymiarów zewnętrznych siłownika ze względów konstrukcyjnych. Wszystkie te prace miały na celu poprawę osiągów silnika spalinowego w szczególności poprawy sprawności w zakresie częściowego obciążenia silnika.
W tym obszarze silnik spalinowy charakteryzuje się stosunkowo niską sprawnością, znacznie odbiegającą od maksymalnej, a jednocześnie w czasie normalnej eksploatacji pojazdów jest obszarem najczęściej eksploatowanym.

Słowa kluczowe: siłownik elektromagnetyczny, regulacja ciśnienia, silnik spalinowy, materiały ferromagnetyczne

Prof. Jarosław Mamala, DSc PhD Eng.

J.Mamala@po.edu.pl

ORCID: 0000-0001-9422-6374

He is employed in the Opole University of Technology in Poland at the Faculty of Mechanical Engineering in the Department of Road Vehicles. He is the author and co-author of several monographs and its scientific achievements attack in more than 220 scientific papers published domestic and foreign SAE, AVEC, FISITA. He has participated in numerous research and development projects of which the most part was the manager. For his scientific achievements received multiple awards e.g. award Patent Office in Poland or the Silver Medal for the invention at the World Exhibition of Innovation, Research and New Technologies Brussels Innova – Eureka Contest and World Exhibition of Innovation in Nuremberg, Geneva. Author and co-author of several patents. Scientifically, he deals with power transfer in the vehicle drive system. For years associated with business, including the technical director of a partner of VW Group. Since 2012 has been President of the Board of Science and Technology Park in Opole. He developed a vision and development strategy for the Park, known as M.I.N.D., which connects the scientific and business community.

Prof. Bronisław Tomczuk, DSc PhD Eng.

B.Tomczuk@po.edu.pl

ORCID: 0000-0002-2042-7170

He received his PhD and DSc Degrees from the Technical University of Lodz (Poland) in 1985 and 1995, respectively. Prior to that, in 1977 he received the MSc Degree in Electrical Engineering with Honours. In 1996 he advanced to the position of Opole University of Technology (OUT) Professor. In 2007 he was promoted to the title of Full Professor in Technical Sciences. It is life title given by the President of the Republic of Poland. His research activity within the Department of Electrical Engineering & Mechatronics is concerned with mathematical modelling of electromagnetic fields in 2D and 3D using the numerical methods for the computer aided design (CAD) of electromagnetic systems. This research is also devoted to the analysis of the dynamics of the mechatronic systems. The objects under consideration are: special transformers and chokes, electromagnetic actuators, active and passive magnetic bearings. He invented 15 constructions of the objects which have been patented since 1995. He is an author of more than 300 publications including books, monographs, papers, and patents as well as grant reports. He has been involved in: Polish Academy of Sciences into: The Electrical Engineering Committee, The Katowice Section of The of Electronics Committee. He has been a member of IEEE and New York Academy of Sciences, and Compumag Society (London) since 2007, 1997 and 2001, respectively. He has been a Member of the Polish Electrical Engineers Association since 1977 and 1986, respectively .

Prof. Andrzej Waindok, DSc PhD Eng.

A.Waindok@po.edu.pl

ORCID: 0000-0002-5921-3583

He received MSc and PhD in Electrical Engineering from the Opole University of Technology (OUT), Poland, in 2002 and 2008, respectively. In 2014, he received the Doctor of Science degree from Faculty of Electrical Engineering, Automatic Control and Informatics at the OUT. Since 2017, he has been a Professor at the Department of Electrical Engineering and Mechatronics at the OUT. He is interested in the mathematical modelling of electromagnetic and thermal fields and its application in computer-aided design of actuators, accelerators, transformers and induction heating systems. He creates 2D and 3D models of linear actuators, railguns, transformers and inductors by using the analytical and numerical methods. He is a member of IEEE since 2007, Polish Electrical Engineers Association since 2001 and Polish Society for Theoretical and Applied Electrical Engineering since 2008.

Mariusz Graba, PhD Eng.

M.Graba@po.edu.pl

ORCID: 0000-0002-3559-0405

He is a graduate of the Faculty of Electrical Engineering of the Opole University of Technology, specializing in Automation and Electrical Metrology. After graduation, he started working as an electronic engineer at the Department of Road and Agricultural Vehicles at the Faculty of Mechanical Engineering of the Opole University of Technology. In 2014, he obtained a PhD in technical sciences in the discipline of Automation and Robotics at the Faculty of Electrical Engineering of the Opole University of Technology. Currently, he works as an assistant professor at the Department of Vehicles at the Faculty of Mechanical Engineering of the Opole University of Technology. Areas of scientific interest include: measurement systems and techniques, vehicle diagnostics and mechatronic systems, programming of microcontrollers, data buses, identification and modeling of control objects, synthesis of control algorithms.

Krzysztof Prażnowski, PhD Eng.

K.Praznowski@po.edu.pl

ORCID: 0000-0002-9008-0635

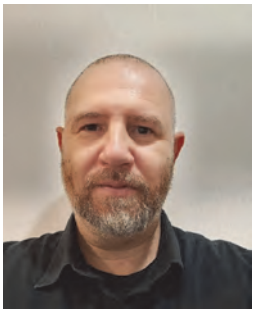

He is research and teaching employee of the Opole University of Technology, Faculty of Mechanical Engineering, Department of Vehicles. The scientific research conducted concerns the analysis of design development and diagnostics of vehicles and machines. The main scope of work carried out concerns signal analysis and digital modeling of mechanical systems.